www.sciencemag.org/content/342/6163/1243/suppl/DC1

Supplementary Materials for

Nonredundant Function of Soluble LTα_3 Produced by Innate Lymphoid Cells in Intestinal Homeostasis

Andrey A. Kruglov,* Sergei I. Grivennikov, Dmitry V. Kuprash, Caroline Winsauer, Sandra Prepens, Gitta Maria Seleznik, Gerard Eberl, Dan R. Littman, Mathias Heikenwalder, Alexei V. Tumanov, Sergei A. Nedospasov*

*Corresponding author. E-mail: andrey_krugloff@mail.ru (A.A.K.); sergei@nedos.net (S.A.N.)

Published 6 December 2013, *Science* **342**, 1243 (2013)
DOI: 10.1126/science.1243364

This PDF file includes:

Materials and Methods

Figs. S1 to S10

Table S1

References

Materials and methods

Mice

$LT\alpha^{f/f}$, $LT\alpha^{\Delta ILC,\ T}$, $LT\beta^{\Delta ILC,\ T}$ and $LT\alpha^{\Delta T}$ were generated during this study. $LT\beta^{f/f}$, TNF KO, $LT\alpha^{-/-}$, TNFR1 KO and TNFR2 KO mice were described elsewhere *(19, 20, 31-33, 34 , 35, 36)*. $TCR\alpha\beta^{-/-}$, $IL10^{-/-}$ were provided by Dr. S. Fillatreau (DRFZ, Germany); $CD40L^{-/-}$ KO mice were provided by Dr. A. Thiel (BCRT, Germany). $TCR\beta\delta^{-/-}$ mice were purchased from Jackson laboratory. $LT\beta^{\Delta ILC,\ T}$ $TCR\alpha\beta^{-/-}$, $LT\beta^{\Delta ILC,\ T}$ $TCR\beta\delta^{-/-}$, $LT\alpha^{-/-}$IL-$10^{-/-}$ mice were generated during this study. All mice were bred and kept under pathogen free conditions. Littermate controls ($LT\beta^{f/f}$ and $LT\alpha^{f/f}$, respectively) were used as wild type controls. All animal procedures were approved and carried out in accordance with national regulations for animal protection.

Bone marrow transfer experiments

Bone marrow chimeras were set up as follows: bone marrow cells were isolated from C57BL/6, TNFR1 KO and TNFR2 KO, $LT\alpha^{\Delta ILC,\ T}$, $LT\beta^{\Delta ILC,\ T}$ and $LT\alpha^{\Delta T}$ mice and 3×10^6 bone marrow cells from each donor were injected into lethally irradiated recipients (10 cagy) 24 hr after irradiation. Analysis of IgA in chimeric mice was performed 6 weeks after transfer.

In vivo manipulations

To activate CD40 signaling, WT and $LT\alpha^{\Delta ILC,\ T}$ mice were injected with 100 mg agonistic anti-CD40 (FGK45) three times on day 0, 2 and 4. Two weeks after first

injection, mice were analyzed for IgA production in the gut. For acute dextran sodium sulfate (DSS) colitis induction, mice were treated with 1,5% DSS in drinking water for 5 days and then put back on normal drinking water for last three days. Live splenic TCRβ positive lymphocytes were purified by sorting using FACS Aria cell sorter (BD Bioscience) and 3×10^6 cells were injected intraperitoneally into $LT\beta^{\Delta ILC,\ T}$ $TCR\beta\delta^{-/-}$ recipients.

Flow cytometry

Fc receptors were blocked with antibody 2.4G2 (10 µg/ml), followed by staining with antibodies against various markers. Antibodies against CD45 (30F11), B220 (RA3.6B2), RORγt (Q31-378), CD23 (B3B4) and secondary reagents SA-PE, SA-PerCP, SA-PE-Cy7 and SA-Cy5 were from BD Bioscience. Antibodies against CD11c (N418), CD11b (M1/70.15.11), Gr1 (RB6-8C5), CD4 (GK1.5), IgM (M41), IL7Rα (A7R34), Thy1.2 (HO13.4), CD19 (1D3), IgD (11.26c), CD21 (7G6), MHCII (M5/114), CD44 (IM7) were purified from respective hybridomas and conjugated to fluorochromes at DRFZ, Berlin. Antibodies against CD3 (145-2C11), IgA (11-44-2), CD11c (N418), CD117 (2B8), CCR9 (eBioCW-1.2), LPAM-1 (DATK32), CD103 (2E7), KI67 (SolA15), TCRβ (H57-597) were purchased from eBioscience. Goat polyclonal anti-IgA antibody was purchased from Bethyl laboratories. CCR6 antibody was purchased from RnD Systems. Exclusion of dead cells was achieved by staining with DAPI (Invitrogene), Propidium Iodide (Sigma-Aldrich) or Fixable Viability Dye eFluor® 450/ eFluor® 660 (eBioscience). Surface lymphotoxin was stained using LTβR-Fc IgG fusion protein kindly

provided by Dr. Y.-X. Fu (Chicago, USA), followed by donkey anti-human IgG(H+L) antibodies (Jackson Immunoresearch). Intracellular staining was performed using FOXP3 Fix/Perm Buffer Set (eBioscience). Data were acquired using flow cytometers FACSCalibur, BD Fortessa, FACSCanto and LSRII (all BD Biosciences). Data analysis was performed using FlowJo software (Tree Star, Inc).

Immunofluorescence and immunohistochemical analysis

Intestine pieces were snap-frozen in OCT-compound (Sakura Tec) and horizontal sections (7 µm) were cut. Slides were fixed with ice-cold acetone, blocked with anti-FcγR antibody (2.4G2) in PBS/BSA and stained with antibodies against IgA (Goat polyclonal; Bethyl Laboratories), B220 (RA3-6B2), RORγt (B2D; eBioscience) for 45 min. Slides were washed, counterstained with DAPI, mounted using Fluoromount G (Southern Biotech) and visualized using Carl Zeiss epifluorescent microscope.

Cell isolation

Intestinal lamina propria lymphocytes were isolated as follows: intestines were collected, Peyer's patches were carefully removed and intestines were open longitudinally. Intestines were subsequently incubated in RPMI-1640 containing 5%FCS, and 10 mM EDTA for 15 min. Afterwards, tubes were vigorously shaken and supernatant, containing intraepithelial lymphocytes, was discarded. The procedure was repeated once more. After that, intestines were extensively

washed with RPMI-1640 with 5% FCS and cut into small pieces and incubated in RPMI containing 5% FCS and 0.3 mg/ml of collagenase IV (Sigma-Aldrich) and 0.1 mg/ml DNAse I (Sigma-Aldrich) for 15 min at 37 °C at constant shaking (200 rpm). The resulting cell suspension was collected and the procedure was repeated until complete intestine digestion was achieved. Then, cells were washed several times with RPMI-1640 and resuspended in 30% Percoll and overlaid on 70% Percoll. For analysis of myeloid cell populations, cells were used further directly without gradient. Gradient solutions were spun at 2,000 rpm for 20 min without braking and the interphase, containing mononuclear cells, was recovered. Cells were washed twice with RPMI-1640 and used for further manipulations. Peritoneal exudate cells were collected by washing peritoneal cavity with 10 ml of PBS. Splenocytes were made using 70 μm cell strainer (BD Bioscience), bone marrow cells were isolated by flushing the bone marrow from femurs with 10 ml of PBS/BSA. Red blood cells in splenocyte and bone marrow preparations were lysed with ACK lysis buffer. Mesenteric lymph nodes cells were prepared by organ digestion using collagenase/DNAse.

IgA ELISA

Murine feces were collected, weighed and resuspended in PBS in concentration 1 mg of feces per 10 μl of PBS. Suspensions were centrifuged at 13,000 rpm for 10 min and supernatant was collected for IgA ELISA. Mouse sera were prepared as previously described (*32*). 96-well plates were coated with anti-mouse Ig (H+L) (Southern Biotech) overnight at 4 °C. Plates were then blocked with 5%

PBS/BSA for 1 hr at room temperature and incubated with 100 µl of supernatants overnight at 4 °C. Goat anti-mouse IgA-AP (Southern Biotech) was used as detection antibody. pNPP (Sigma-Aldrich) was used as a substrate. Reaction was stopped by adding 50 µl of 3M NaOH.

Microbiota analysis

Contents from the distal part of the small intestine (ileum) were resuspended in 1 ml of lysis buffer (50 mM Tris-HCl, pH 8.0; 500 mM NaCl; and 50 mM EDTA and 4 % SDS) in Lysing Matrix B tubes (MP Biomedicals). Intestinal bacteria were lysed by mechanical disruption with a bead beater (BioSpec Products) for 1 min and further incubated at 70 °C for 15 min with gentle shaking by hand every 5 min. Supernatant was collected after centrifugation for 5 min at 14,000 rpm and the procedure was repeated once more. Pooled supernatant was mixed with 260 µl of 10M ammonium acetate and incubated on ice for 5 min, centrifuged for 10 min at 14,000 rpm. DNA was precipitated from supernatants by adding an equal volume of isopropanol to each sample and incubation on ice for 15 min. After centrifugation for 15 min at 14,000 rpm, nucleic acid pellets were washed once with 70 % ethanol and dissolved in 100 mcl of TE buffer in the presence of RNAse A (2 µg/ml). For deep sequencing, 16S rRNA was amplified using BSR357 (5'-CCATCTCATCCCTgCgTgTCTCCgACTCAgNNNNCTgCTgCCTYCCgTA) and BSF8 (5'-CCTATCCCCTgTgTgCCTTggCAgTCTCAgAgAgTTTgATCCTggCTCAg). PCR

products were sequenced on a 454 GS FLX platform following the 454 Roche recommended procedures. Classification of bacteria was performed as previously described (*37*, *38*). Microbiota composition was further quantified by Real-time PCR using strain specific primers (Table S1) and was normalized relative to eubacteria.

Induction of IgA switch in vitro

Splenic B cells were isolated using CD19 microbeads (Myltenyi Biotec). Purified B cells (10^5 cells) were cultured for 5 days in the presence of LPS (25 µg/ml; Sigma-Aldrich), recombinant human TGFβ1 (2 ng/ml; RnD systems), recombinant mouse IL-4 (10 ng/ml; RnD systems), and recombinant mouse IL-5 (1,5 ng/ml; Ebioscience). On day 5, cells were harvested and stained for IgM and IgA. Frequencies of IgA positive cells were determined using flow cytometry (LSRFortessa; BD biosciences). For cocultures of B cells and dendritic cells, IgM^+ B cells were purified from spleen using biotinylated anti-IgM (M41) antibody, followed by anti-biotin microbeads (Myltenyi Biotec). Mesenteric lymph node dendritic cells were purified as follows: lymph node was cut into small pieces and digested in the mixture of collagenase IV (Sigma-Aldrich) and DNAse (Sigma-Aldrich). Digested tissue was passed through 18 G and 25 G needles in order to obtain single cell suspension. Cells were washed twice with PBS/BSA and dendritic cells were isolated using anti-CD11c microbeads (Myltenyi Biotech) according to manufacturer's instructions. Cocultures were performed in 96 well

plates with 2×10^5 B cells and 4×10^4 DC per well for 5 days. At day 5, IgA were measured in supernatants.

Real-time PCR

RNA from tissues and cells was isolated using TRI reagent (Sigma-Aldrich) according to manufacturer's instructions. RNA (1 µg) was treated with RQ1 DNAse 1 (Promega Inc.) and cDNA was synthesized using Im-Prom II reverse transcriptase (Promega Inc.). Real-time PCR was performed using Brilliant II SYBR Green QPCR master mix (Agilent). PCR was performed using Stratagene Real-time PCR amplifier. All reactions were run using the following program: 95 °C 10 min; 50 cycles of 95 °C 30 sec, 60 °C 30 sec and 72 °C 30 sec. Sequences of primers are shown in **Table S1**.

Statistical analysis

Statistical analysis was done using two-tailed unpaired Student's T-test unless otherwise stated. P-values ($P< 0.05$) were considered as statistically significant.

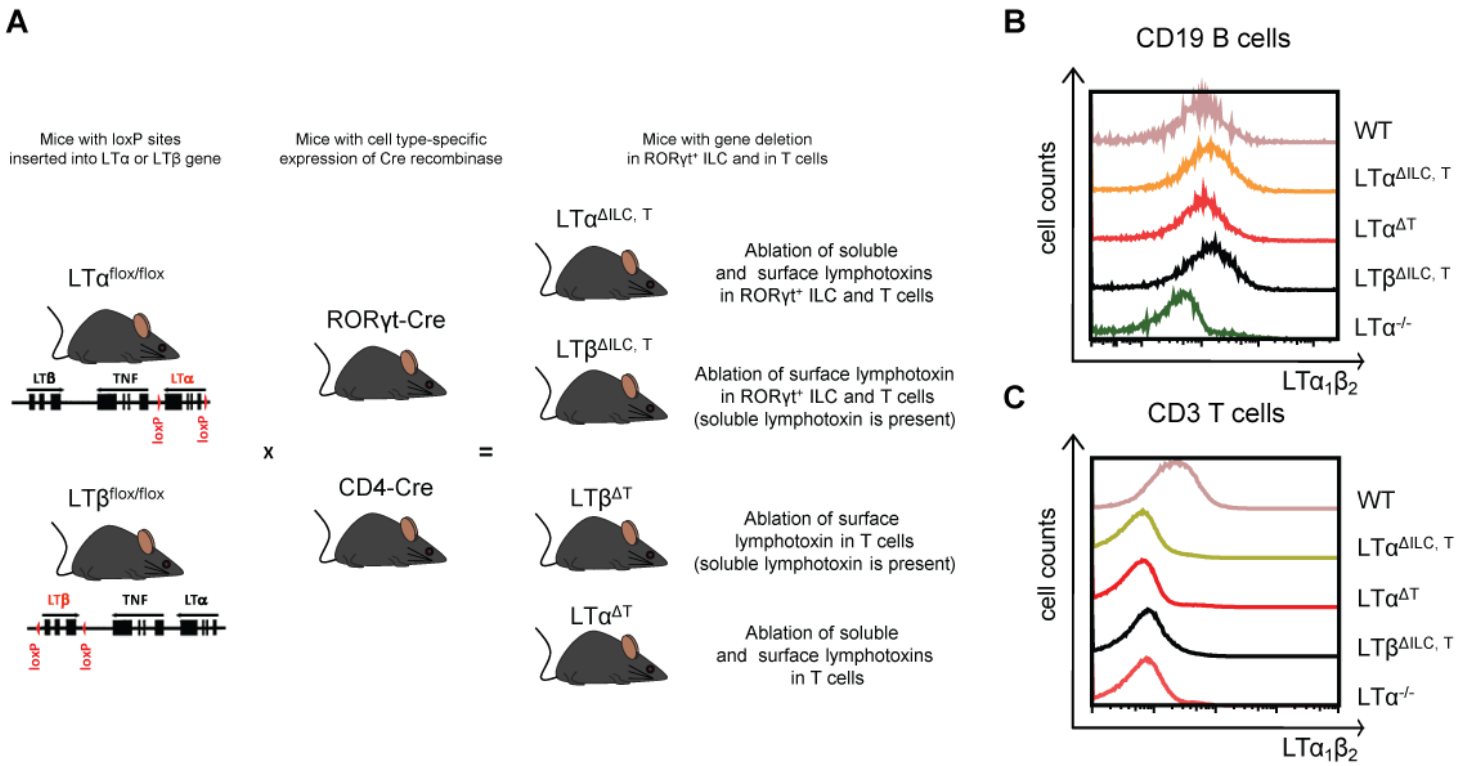
A
Mice with loxP sites inserted into LTα or LTβ gene
Mice with cell type-specific expression of Cre recombinase
Mice with gene deletion in RORγt+ ILC and in T cells
LTα flox/flox
LTβ
TNF
LTα
loxP
loxP
x
RORγt-Cre
=
LTβ flox/flox
CD4-Cre
LTα ΔILC, T
Ablation of soluble and surface lymphotoxins in RORγt+ ILC and T cells
LTβ ΔILC, T
Ablation of surface lymphotoxin in RORγt+ ILC and T cells (soluble lymphotoxin is present)
LTβ ΔT
Ablation of surface lymphotoxin in T cells (soluble lymphotoxin is present)
LTα ΔT
Ablation of soluble and surface lymphotoxins in T cells
B
CD19 B cells
cell counts
WT
LTα ΔILC, T
LTα ΔT
LTβ ΔILC, T
LTα -/-
LTα1β2
C
CD3 T cells
cell counts
WT
LTα ΔILC, T
LTα ΔT
LTβ ΔILC, T
LTα -/-
LTα1β2

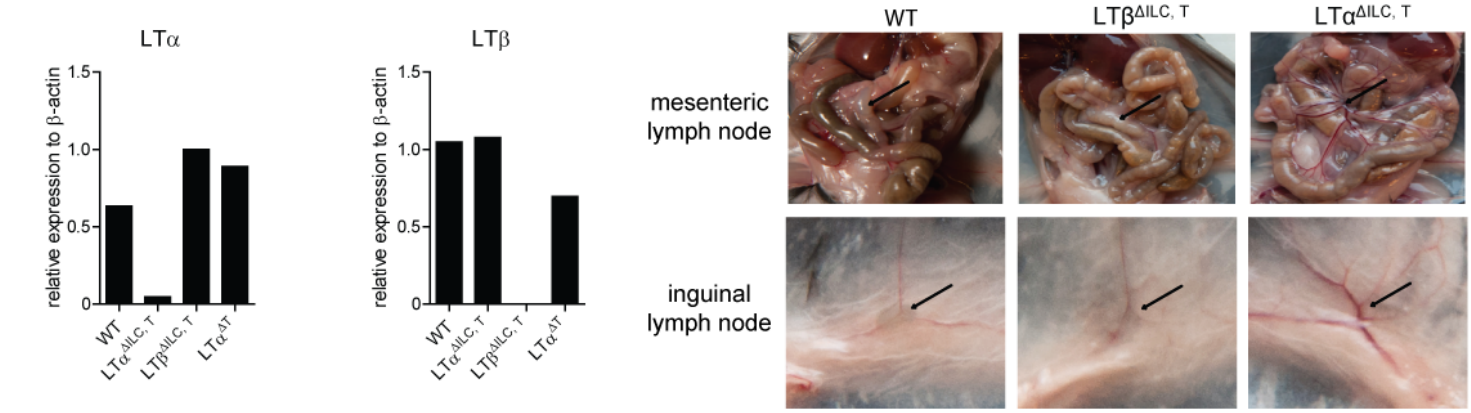
D
LTα
relative expression to β-actin
1.5
1.0
0.5
0
WT
LTα ΔILC, T
LTβ ΔILC, T
LTα ΔT
E
LTβ
relative expression to β-actin
1.5
1.0
0.5
0
WT
LTα ΔILC, T
LTβ ΔILC, T
LTα ΔT
F
WT
LTβ ΔILC, T
LTα ΔILC, T
mesenteric lymph node
inguinal lymph node

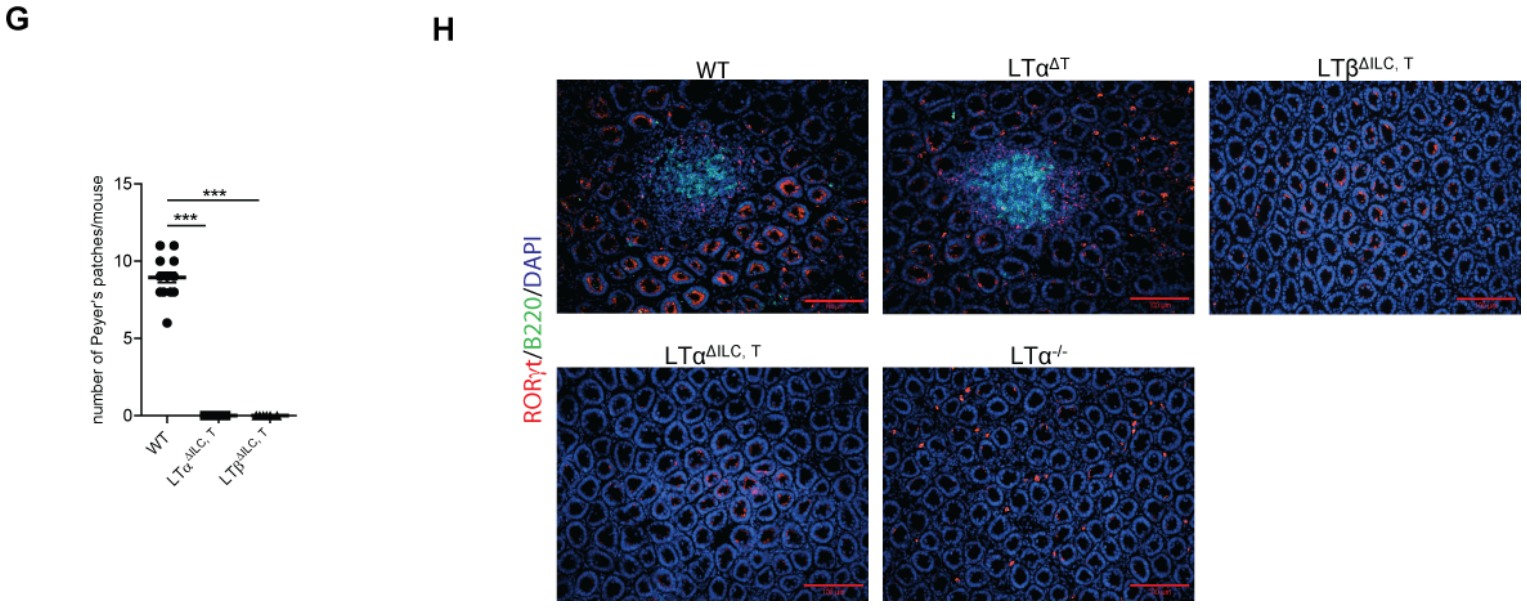
G
number of Peyer's patches/mouse
15
10
5
0
***
***
WT
LTα ΔILC, T
LTβ ΔILC, T
H
WT
LTα ΔT
LTβ ΔILC, T
LTα ΔILC, T
LTα -/-
RORγt/B220/DAPI

Fig. S1. Generation and phenotypic analysis of mice lacking LTα and LTβ in RORγt$^+$ cells. (**A**) Breeding scheme to generate mice lacking LTα and LTβ in T cells and in RORγt$^+$ ILC and T cells. $LT\alpha_1\beta_2$ protein expression on CD19$^+$ B cells (**B**) and CD3$^+$ T cells (**C**) in spleen of WT, $LT\beta^{\Delta ILC,\ T}$ and $LT\alpha^{\Delta ILC,\ T}$, $LT\alpha^{\Delta T}$ and $LT\alpha^{-/-}$ mice. Splenocytes ($1x10^6$) were activated with PMA (50 ng/ml) and anti CD40 (10 μg/ml) antibodies for 7 hours. Cells were stained with LTβR-hIgG, followed by donkey anti-human IgG (H+L) and surface markers. Expression of LTα (**D**) and LTβ (**E**) mRNA in sorted CD4$^+$IL7Rα$^+$lin(CD3/B220/CD11c)$^-$ splenic ILC from WT, $LT\beta^{\Delta ILC,\ T}$ and $LT\alpha^{\Delta ILC,\ T}$, $LT\alpha^{\Delta T}$ mice. (**F)** Development of mesenteric and inguinal lymph nodes in WT, $LT\beta^{\Delta ILC,\ T}$ and $LT\alpha^{\Delta ILC,\ T}$ mice. (**G**) Numbers of Peyer's patches in WT, $LT\beta^{\Delta ILC,\ T}$ and $LT\alpha^{\Delta ILC,\ T}$ mice. (**H**) $LT\alpha_1\beta_2$ expressed by RORγt$^+$ ILC is critical for ILF development in the gut. Horizontal sections of small intestine were stained for RORγt (green) and B220 (red) and counterstained with DAPI (blue). Scale bar, 100μm. Original magnification × 400. All data are representative of two or more independent experiments with $n \geq 3$ mice. *P<0.05, **P<0.01, ***P<0.001, as calculated by Students' t-test.

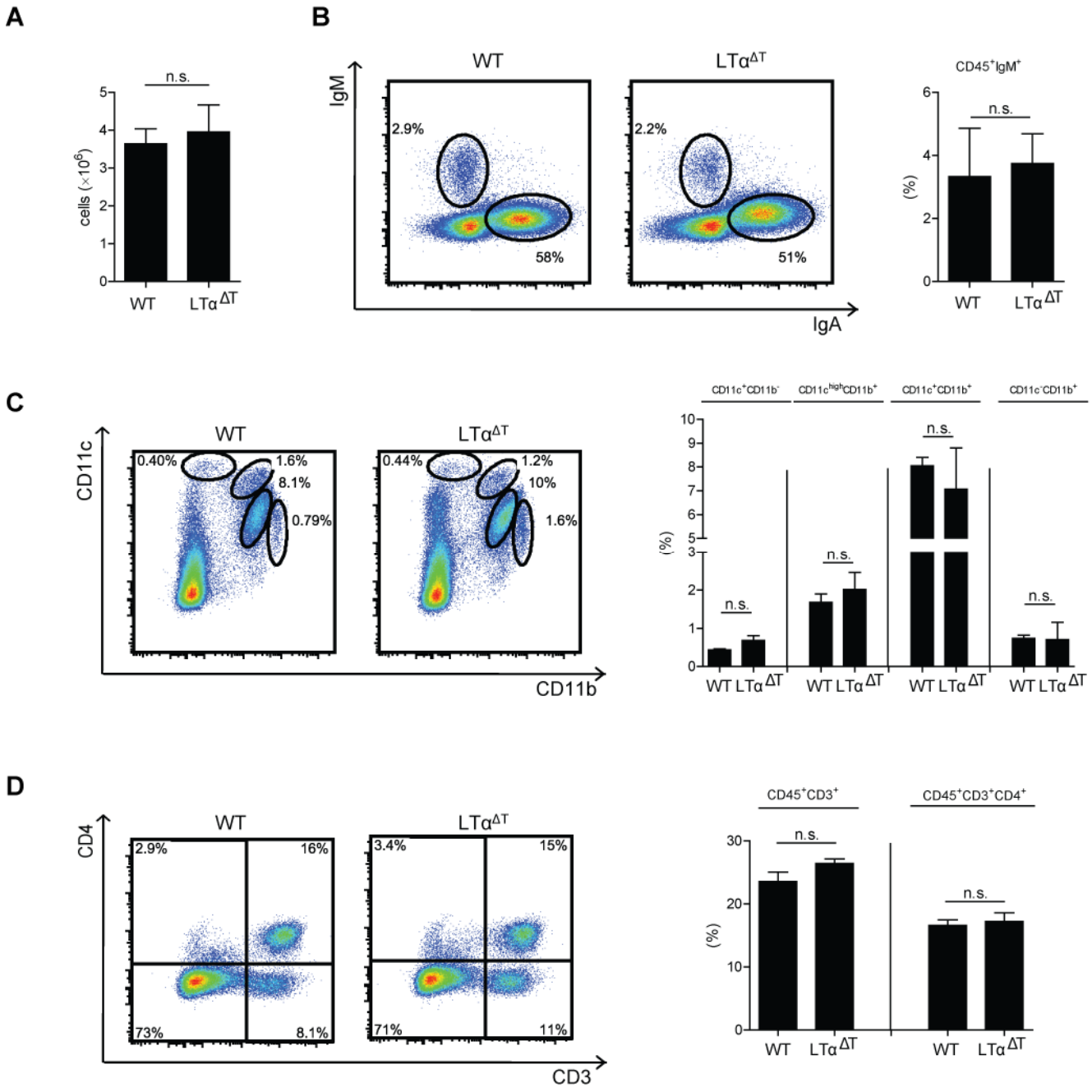

Fig. S2. Lymphocyte populations in the lamina propria after ablation of LTα in T cells. (**A**) Lamina propria cell numbers in WT and LTα$^{\Delta T}$ animals. (**B**) IgM and IgA producing B cells in the CD45^{+} susbet of lamina propria lymphocytes isolated from WT and LTα$^{\Delta T}$ animals. (**C**) Frequencies of various myeloid cell

populations in live CD45^{+} lamina propria cells of WT and LTα$^{\Delta T}$ animals (right) as determined by surface expression of CD11c and CD11b (left). (**D**) Analysis of T cell subsets in CD45^{+} subset of lamina propria lymphocytes isolated from WT and LTα$^{\Delta T}$ animals. All data are representative of two independent experiments with $n \geq 3$. *$P<0.05$, **$P<0.01$, ***$P<0.001$, as calculated by Students' *t*-test.

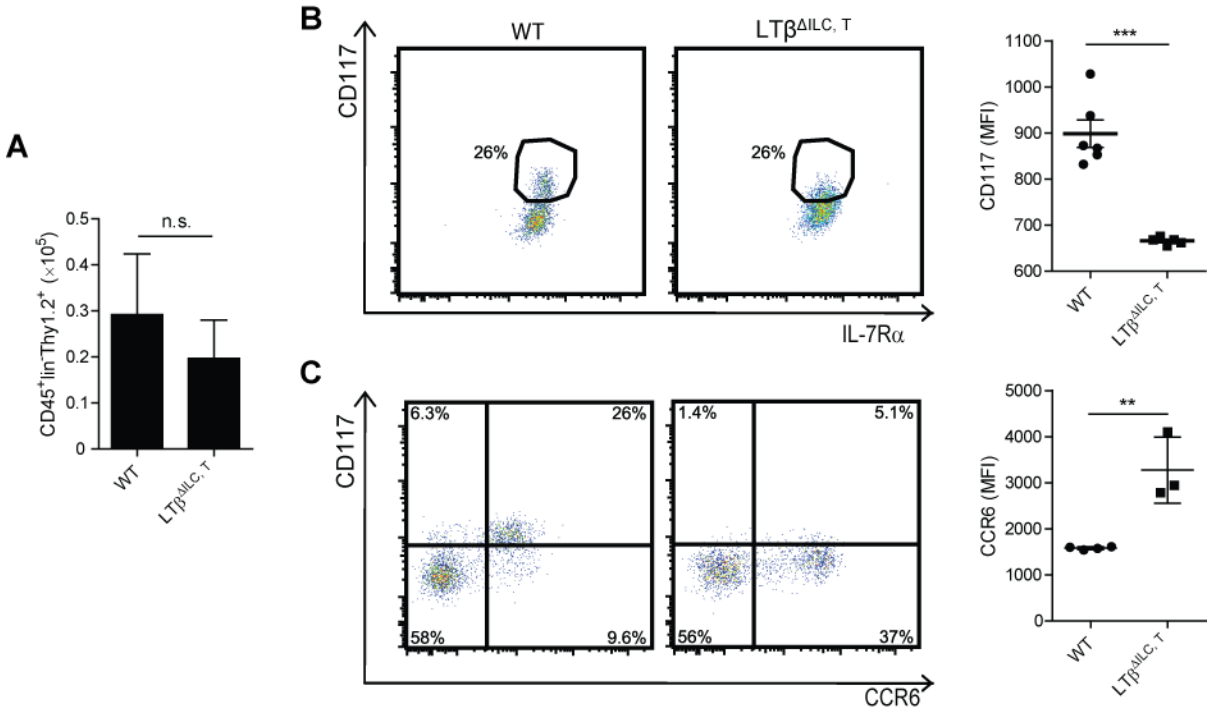

Fig. S3. Control of RORγt$^+$ ILC lamina propria phenotype by LTα$_1$β$_2$ produced by RORγt$^+$ ILC. (**A**) Cell numbers of CD45$^+$lin(CD3/B220/CD11c)$^-$ Thy1.2$^+$ cells in the lamina propria of WT and LTβ$^{\Delta ILC,\ T}$ animals. Analysis of CD117 (**B**), IL-7Rα and CCR6 (**C**) expression on CD45$^+$ lin$^-$ Thy1.2$^+$ cells in the lamina propria of WT and LTβ$^{\Delta ILC,\ T}$ animals. Lamina propria cells were gated on CD45$^+$lin$^-$Thy1.2$^+$ and expression CD117, IL-7Rα and CCR6 was analyzed. All data are representative of at least two independent experiments with n≥3 mice. Error bars, SEM; *P<0.05, **P<0.01, ***P<0.001, as calculated by Student's t-test.

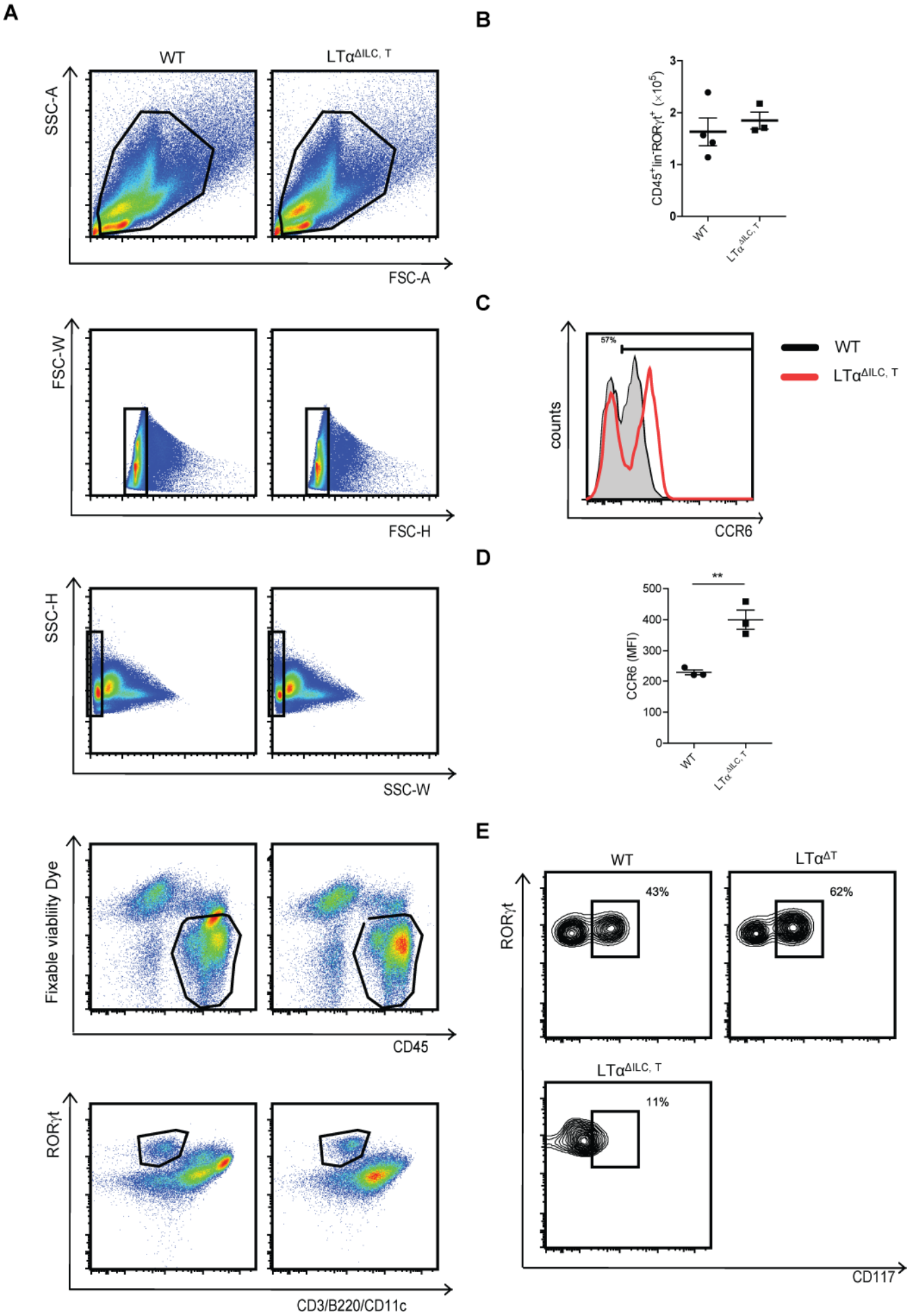
A
WT
LTα^ΔILC, T
SSC-A
FSC-A
FSC-W
FSC-H
SSC-H
SSC-W
Fixable viability Dye
CD45
RORγt
CD3/B220/CD11c
B
CD45+lin-RORγt+ (×10^5)
3
2
1
0
WT
LTα^ΔILC, T
C
57%
counts
CCR6
WT
LTα^ΔILC, T
D
**
CCR6 (MFI)
500
400
300
200
100
0
WT
LTα^ΔILC, T
E
WT
LTα^ΔT
43%
62%
LTα^ΔILC, T
11%
RORγt
CD117

Fig. S4. Analysis of lamina propria ILC compartment upon LTα ablation in RORγt^{+} cells. (**A**) Gating strategy for quantification of RORγt^{+} ILC located in the lamina propria. (**B**) Cell numbers of RORγt^{+} ILC in the lamina propria of WT and LTα$^{\Delta ILC,\ T}$ mice. (**C**, **D**). CCR6 expression on RORγt^{+} ILC, gated as shown in A, in WT and LTα$^{\Delta ILC,\ T}$. (**E**) CD117 (c-Kit) expression on RORγt^{+} ILC, gated as shown in A, in WT, LTα$^{\Delta T}$ and LTα$^{\Delta ILC,\ T}$ mice. All data are representative of two or more independent experiments with $n \geq 3$ mice. Error bars, SEM; *P<0.05, **P<0.01, ***P<0.001, as calculated by Student's t-test.

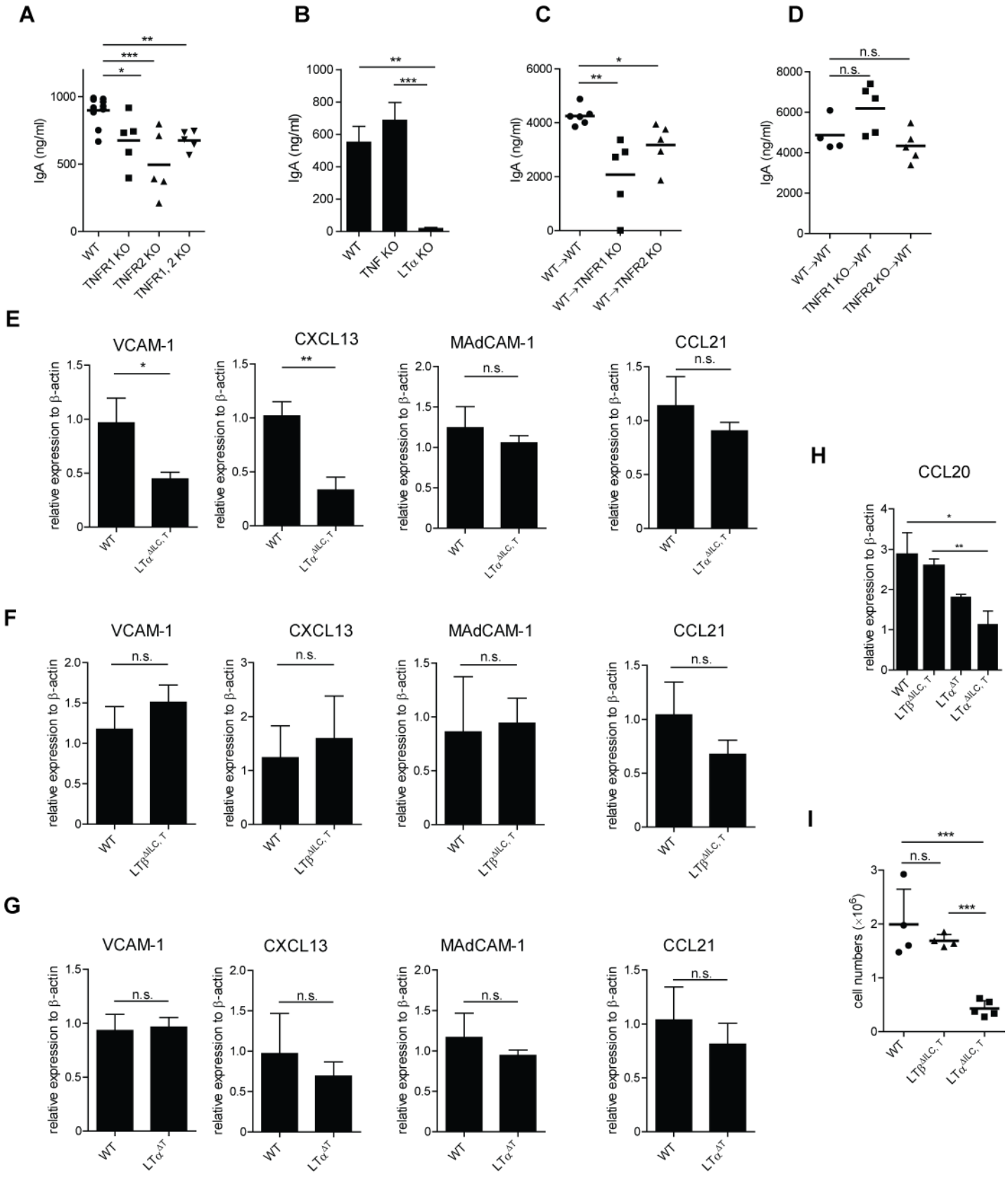
A
IgA (ng/ml)
WT
TNFR1 KO
TNFR2 KO
TNFR1, 2 KO
B
IgA (ng/ml)
WT
TNF KO
LTα KO
C
IgA (ng/ml)
WT→WT
WT→TNFR1 KO
WT→TNFR2 KO
D
IgA (ng/ml)
n.s.
WT→WT
TNFR1 KO→WT
TNFR2 KO→WT
E
VCAM-1
CXCL13
MAdCAM-1
CCL21
relative expression to β-actin
WT
LTα ΔILC, T
F
VCAM-1
CXCL13
MAdCAM-1
CCL21
relative expression to β-actin
WT
LTβ ΔILC, T
G
VCAM-1
CXCL13
MAdCAM-1
CCL21
relative expression to β-actin
WT
LTα ΔT
H
CCL20
relative expression to β-actin
WT
LTβ ΔILC, T
LTα ΔT
LTα ΔILC, T
I
cell numbers (×10^6)
WT
LTβ ΔILC, T
LTα ΔILC, T

Fig. S5. Role of TNFR1, TNFR2 and soluble lymphotoxin in the control of IgA induction and intestinal chemokine production. (**A**) Reduced fecal IgA levels in TNFR1 KO, TNFR2 KO and TNFR1, 2 KO animals. (**B**) Normal fecal IgA levels in TNF deficient mice. (**C**) Reduced fecal IgA levels in TNFR1 KO and TNFR2 KO mice reconstituted with WT bone marrow. (**D**) Normal fecal IgA levels in WT animals reconstituted with TNFR1 KO and TNFR2 KO bone marrow cells. (**E**) Chemokine expression in jejunum of WT and $LT\alpha^{\Delta ILC,\ T}$ animals. (**F**) Chemokine expression in jejunum of WT and $LT\beta^{\Delta ILC,\ T}$ animals. (**F**) Chemokine expression in jejunum of WT and $LT\alpha^{\Delta T}$ animals. (**G**) Expression of CCL20 in jejunum of WT, $LT\alpha^{\Delta ILC,\ T}$, $LT\beta^{\Delta ILC,\ T}$ and $LT\alpha^{\Delta T}$ animals. (**H**) Lamina propria lymphocyte cell numbers in WT, $LT\beta^{\Delta ILC,\ T}$ and $LT\alpha^{\Delta ILC,\ T}$ mice. All data are representative of two or more independent experiments with $n \geq 3$ mice. Error bars, SEM; *$P<0.05$, **$P<0.01$, ***$P<0.001$, as calculated by Student's *t*-test.

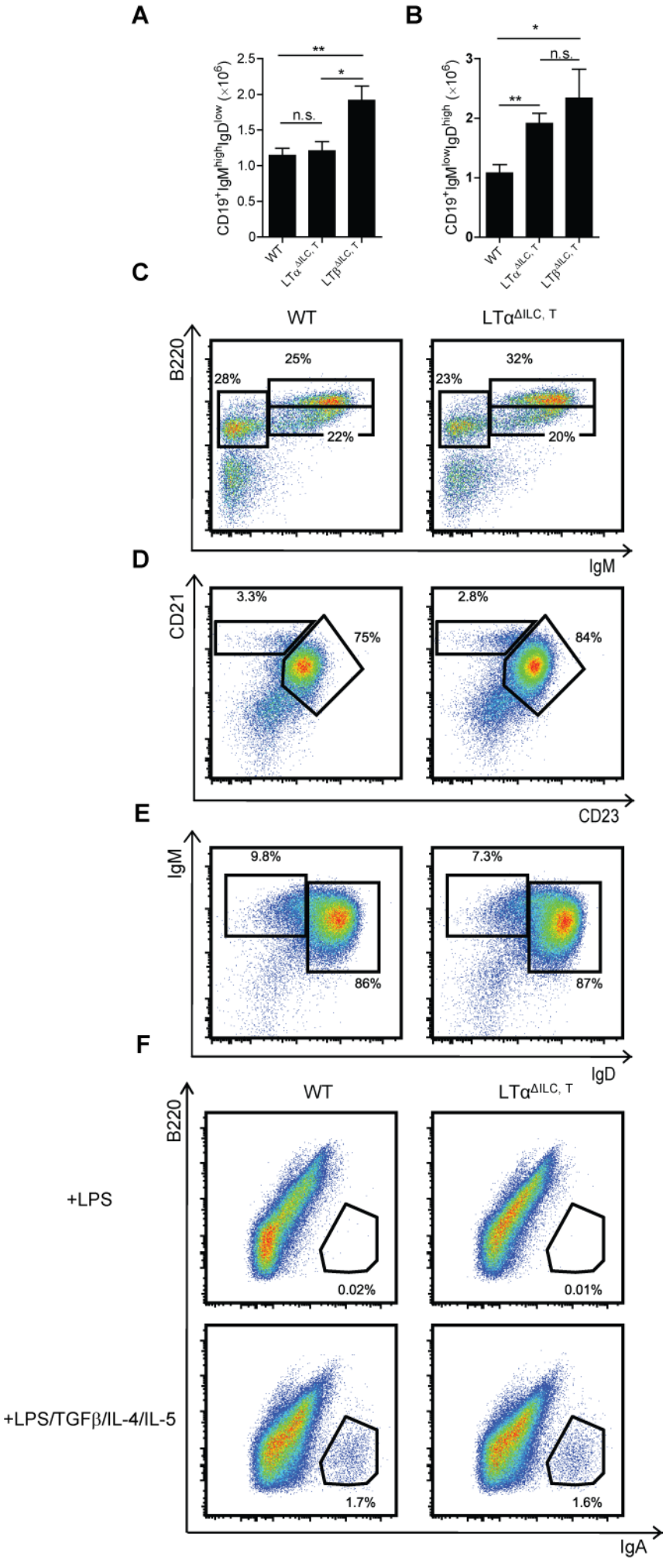
A
B
C
D
E
F
CD19+IgMhighIgDlow (×10^6)
CD19+IgMlowIgDhigh (×10^6)
n.s.
**
*
WT
LTα^ΔILC, T
LTβ^ΔILC, T
B220
IgM
CD21
CD23
IgD
IgA
25%
28%
22%
32%
23%
20%
3.3%
75%
2.8%
84%
9.8%
86%
7.3%
87%
+LPS
+LPS/TGFβ/IL-4/IL-5
0.02%
0.01%
1.7%
1.6%

Fig. S6. B cell development upon LT ablation in RORγt^{+} cells. (**A**, **B**) B1 ($CD19^{+}IgM^{high}IgD^{low}$) and B2 ($CD19^{+}IgD^{high}IgM^{low}$) cell numbers in peritoneal cavity of WT, $LT\beta^{\Delta ILC,\ T}$ and $LT\alpha^{\Delta ILC,\ T}$ mice. (**C**) Frequencies of pre/pro-B ($B220^{+}IgM^{-}$), immature ($B220^{lo}$, IgM^{+}) and mature recirculating ($B220^{hi}$, IgM^{+}) B cells in bone marrow of WT and $LT\beta^{\Delta ILC,\ T}$ animals. (**D**) Frequencies of follicular ($B220^{+}CD21^{+}CD23^{+}$) and marginal zone ($B220^{+}CD21^{+}CD23^{-}$) B cells in spleen of WT and $LT\alpha^{\Delta ILC,\ T}$ animals. (**E**) Frequencies of $IgM^{hi}IgD^{lo}$, $IgM^{+}IgD^{+}$ B cells in spleen of WT and $LT\alpha^{\Delta ILC,\ T}$ animals. (**F**) B cells were isolated from spleen of WT and $LT\alpha^{\Delta ILC,\ T}$ animals and were cultured for 5 days in presence of lipopolysaccharide (LPS) only or LPS, rhTGFβ, rmIL-4 and rmIL-5. Cells were stained with B220 and IgA and the frequency of IgA^{+} cells was determined by FACS analysis.

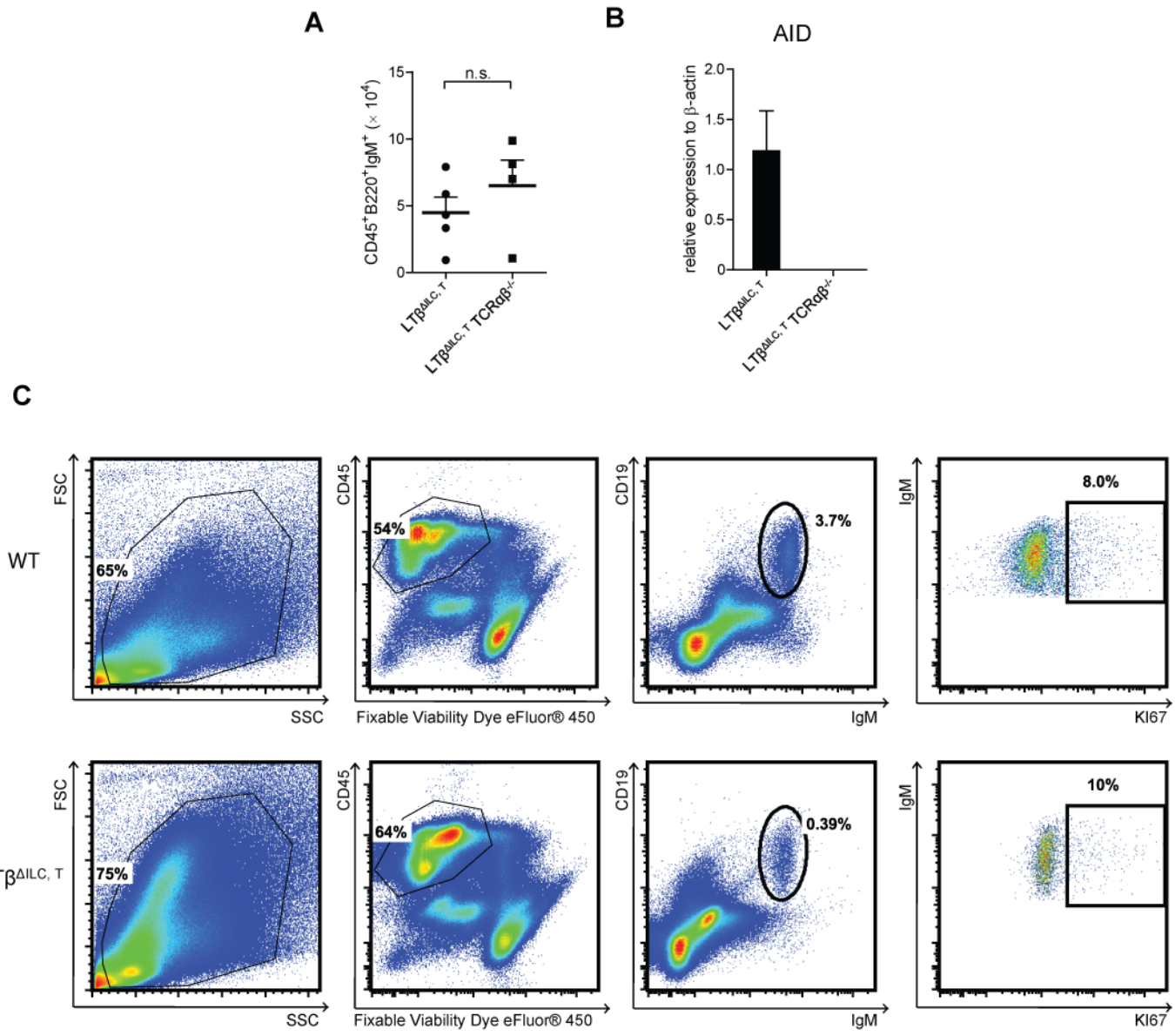

Fig. S7. Analysis of B cell proliferation and AID expression in the lamina propria in LTβ$^{\Delta ILC,\ T}$ mice. (**A**) Numbers of lamina propria IgM^{+} B cells in LTβ$^{\Delta ILC,\ T}$ and LTβ$^{\Delta ILC,\ T}$ TCRαβ$^{-/-}$ mice. (**B**) AID expression in lamina propria lymphocytes isolated from the small intestine of LTβ$^{\Delta ILC,\ T}$ and LTβ$^{\Delta ILC,\ T}$ TCRαβ$^{-/-}$ mice. (**C**) Lamina propria cells were isolated from the small intestine of WT and LTβ$^{\Delta ILC,\ T}$ mice and stained for surface CD45, CD19, IgM and intracellularly for KI67. Dead

cells were excluded using fixable Viability Dye eFluor 450. All data are representative of two independent experiments. Error bars, SEM; *P<0.05, **P<0.01, ***P<0.001, as calculated by Student's t-test.

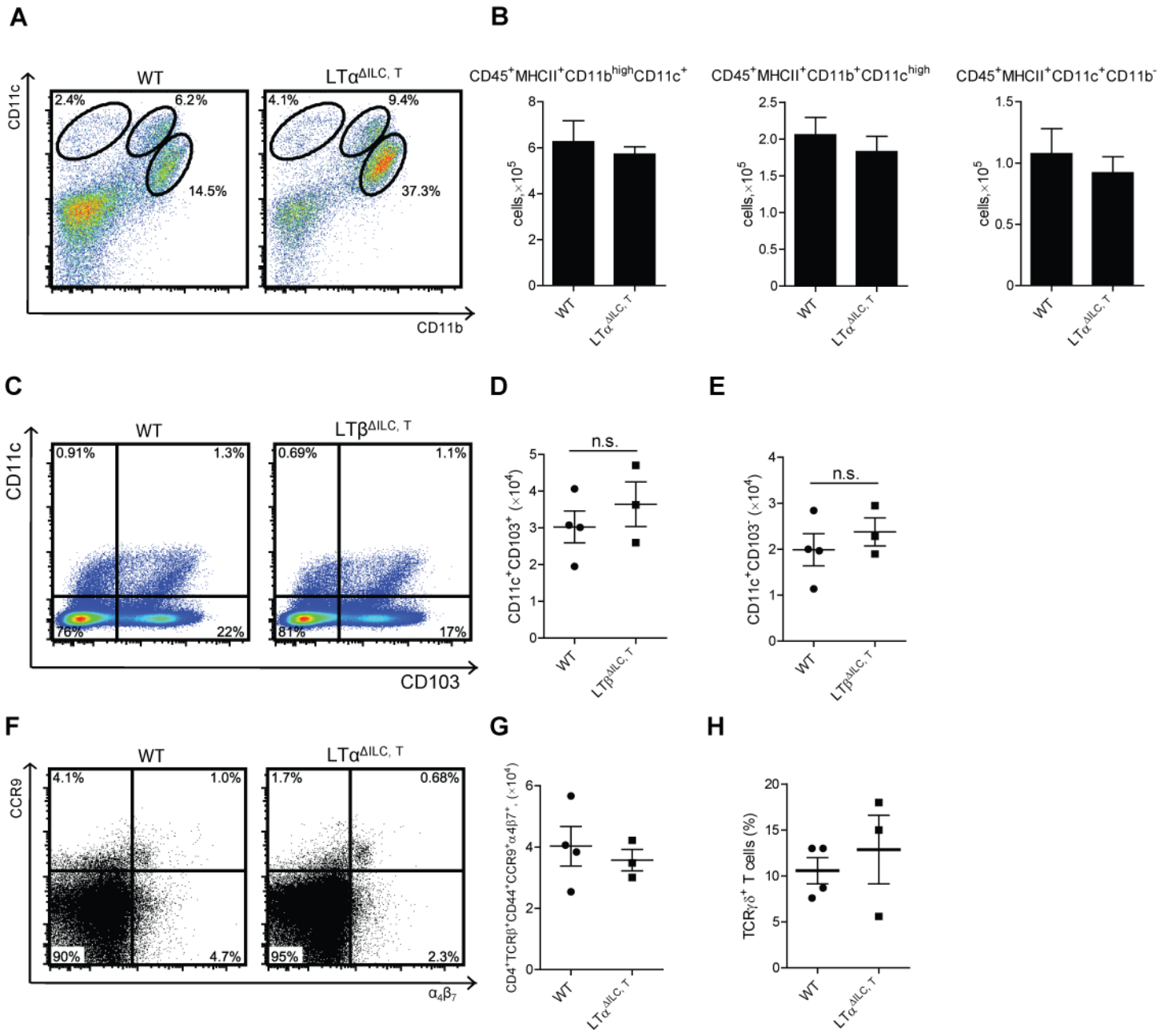

Fig. S8. Analysis of cell populations in gut-associated lymphoid tissues upon LT ablation in RORγt$^+$ cells. (**A**) Representative flow cytometry dot plots of live CD45$^+$MHCII$^+$ lamina propria lymphocytes in WT and LTα$^{\Delta ILC, T}$ animals. (**B**) Cell numbers of various dendritic cell populations in the lamina propria of WT and LTα$^{\Delta ILC, T}$ mice. (**C**) Representative flow cytometry dot plots of

$CD11c^+CD103^+$ lymphocytes from mesenteric lymph nodes in WT and $LT\beta^{\Delta ILC,\ T}$ animals. (**D**) Cell numbers of $CD11c^+CD103^+$ and $CD11c^+CD103^-$ in mesenteric lymph nodes of WT and $LT\beta^{\Delta ILC,\ T}$ mice. (**E**) Expression of CCR9 and $\alpha_4\beta_7$ in splenic $CD4^+TCR\beta^+CD44^+$ T cells in WT and $LT\alpha^{\Delta ILC,\ T}$ animals. (**F**). Cellular numbers of $CD4^+TCR\beta^+CD44^+CCR9^+\alpha_4\beta_7{}^+$ T cells in spleen of WT and $LT\alpha^{\Delta ILC,\ T}$ mice. All data are representative of two independent experiments with $n \geq 3$ mice. Error bars, SEM; **P*<0.05, ***P*<0.01, ****P*<0.001, as calculated by Student's *t*-test.

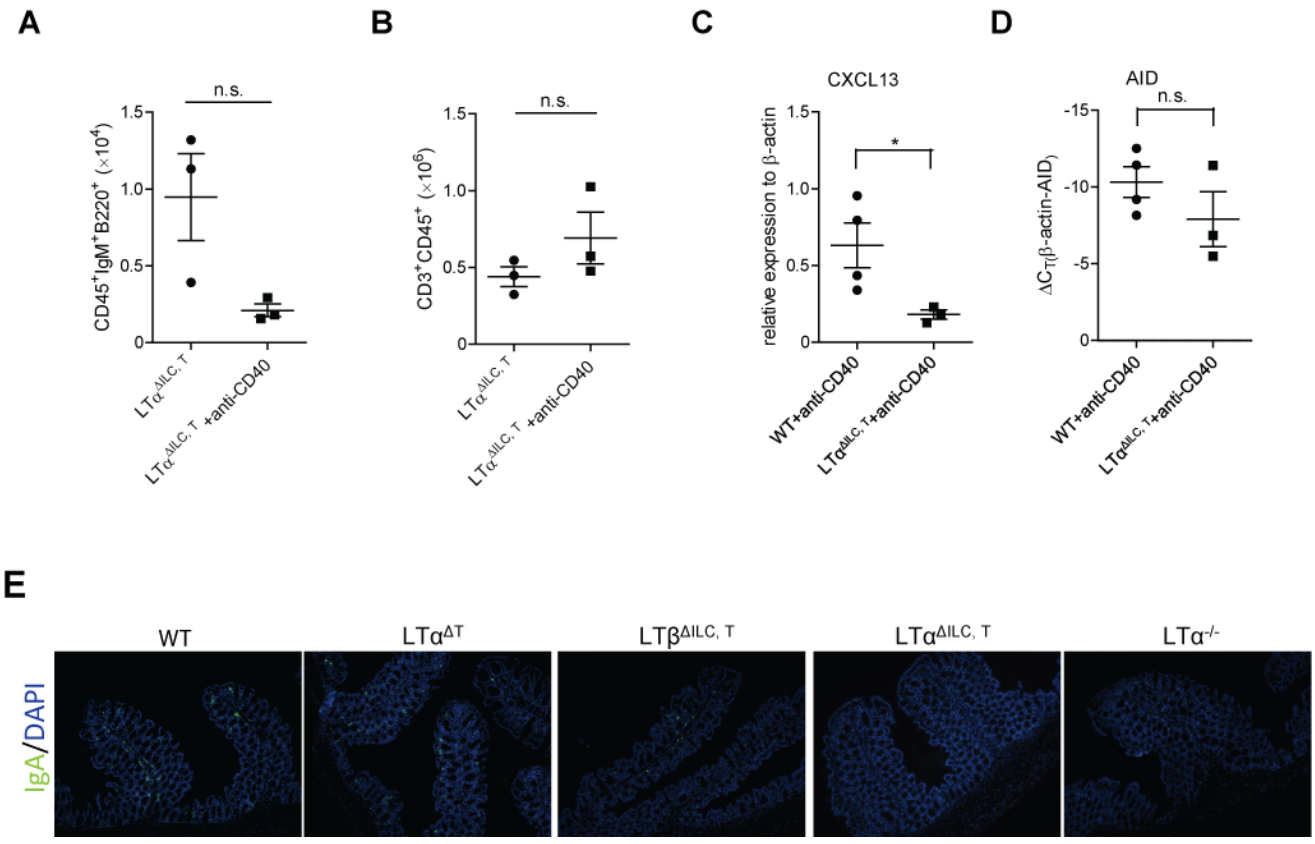

Fig. S9. Induction of IgA production in mice lacking LTα in RORγt^{+} cells. (**A**) Numbers of live lamina propria B cells (CD45^{+}IgM^{+}B220^{+}) in the LP of untreated or anti-CD40-treated LTα$^{\Delta ILC, T}$ 2 days after single antibody injection. (**B**) Numbers of live lamina propria T cells (CD45^{+}CD3^{+}) in the lamina propria of untreated or anti-CD40-treated LTα$^{\Delta ILC, T}$ 2 days after single antibody injection. (**C**) CXCL13 expression in small intestine of anti-CD40-treated WT and LTα$^{\Delta ILC, T}$ 2 days after single antibody injection. (**D**) AID expression in lamina propria lymphocytes isolated from anti-CD40-treated WT and LTα$^{\Delta ILC, T}$ 2 days after single antibody injection. (**E**) Analysis of IgA producing cells in colons of dextran sodium sulfate (DSS) -treated WT, LTα$^{\Delta T}$, LTα$^{\Delta ILC, T}$ LTβ$^{\Delta ILC, T}$, LTα$^{-/-}$ mice. Immunofluorescent analysis of colon of WT, LTα$^{\Delta T}$, LTα$^{\Delta ILC, T}$ LTβ$^{\Delta ILC, T}$, LTα$^{-/-}$

mice at day 8 after DSS treatment. Mice were treated with 1,5 % DSS in drinking water for 5 days and then put back on normal drinking water. On day 8, colons were collected and analyzed by immunofluorescence on the presence of IgA^+ cells. IgA^+ cells (green) were observed only in WT, $LT\alpha^{\Delta T}$, $LT\beta^{\Delta ILC,\ T}$ animals. All data are representative of two independent experiments with $n \geq 3$ mice. Error bars, SEM; *P<0.05, **P<0.01, ***P<0.001, as calculated by Student's t-test.

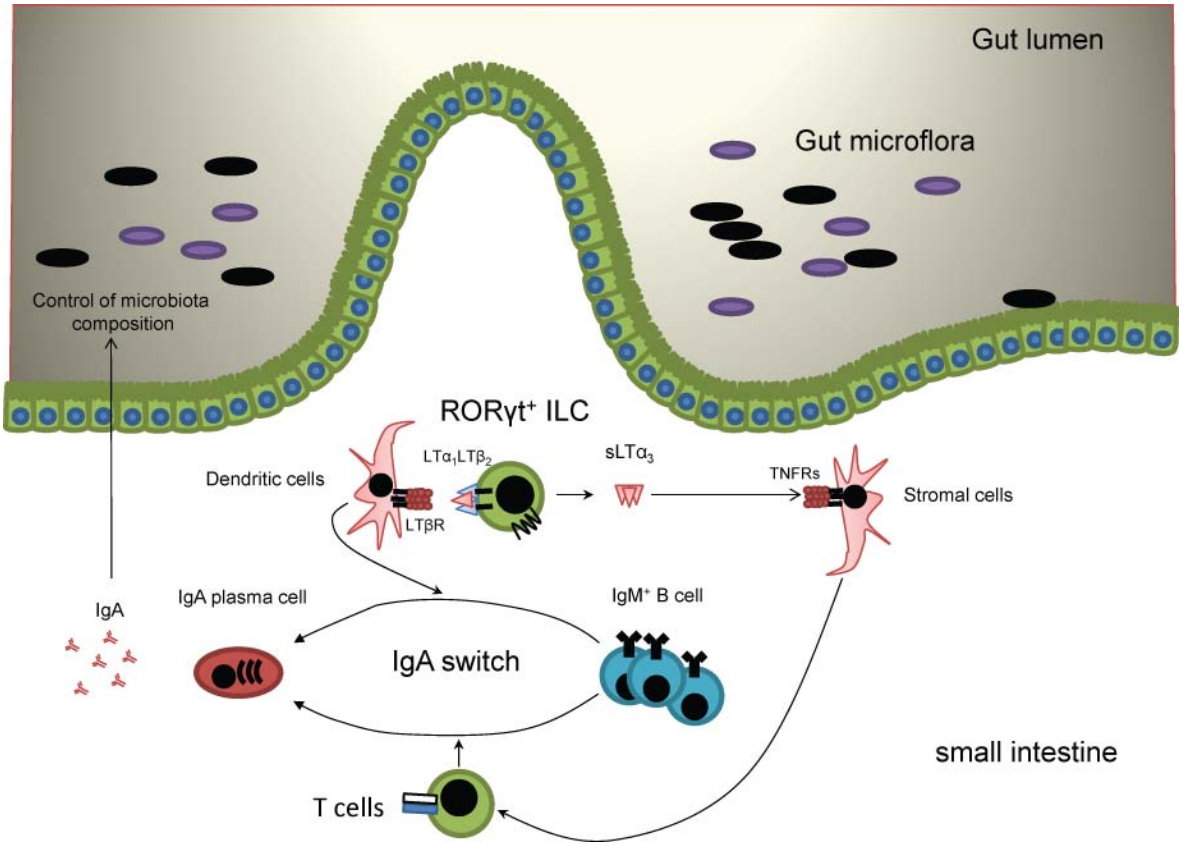

Fig. S10. Soluble and membrane-bound lymphotoxins expressed by innate lymphoid cells distinctly orchestrate intestinal homeostasis. This study identifies that ILC via their production of soluble and membrane-bound lymphotoxin regulate distinct pathways of IgA induction and, thereby, orchestrate intestinal homeostasis. The nonredundant pathway controlled by soluble LTa is shown on the right.

Table S1. Primer sequences used for Real-time PCR

Gene	Forward primer	Reverse primer
AID	gCCACCTTCgCAACAAgTCT	CCgggCACAgTCATAgCAC
CXCL13	ggCCACggTATTCTggAAgC	gggCgTAACTTgAATCCgATCTA
CCL21	ATCCCggCAATTCCTgTTCTC	ggggCTTTgTTTCCCTggg
MAdCAM-1	CTgAgCCCTACATCCTgACCT	gCTTCACAgAgTAgCTCCCAg
LTα	ATTCTAAAgAAACCCAAgAATTg	CAACCTTCCCCTgTTCCCA
LTβ	ACgTCgggTTgAgAAgATCA	TggATCTggTgTAgAATCCg
VCAM-1	ggCTCCAgACATTTACCCAgT	ACCCTTgAACAgATCAATCTCCA
CCL20	CTTCATCggCCATCTgTCTT	ggTACTgCTggCTCACCTCT
CD40L	CCTTgCTgAACTgTgAggAgA	CTTCgCTTACAACgTgTgCT
INOS	ATgCTgCCACCTTggAgTTCAC	ggCCACCCACCTCCAgTAgC
β-actin	CTCCTgAGCgCAAGTACTCTgTg	TAAAACgCAgCTCAgTAACAgTCC
Eubacteria	ACTCCTACgggAggCAgCAgT	ATTACCgCggCTgCTggC
Segmentous fillamented bacteria	gACgCTgAggCATgAgAgCAT	gACggCACggATTgTTATTCA
Lactobacteria	AgCAgTAgggAATCTTCCA	CACCgCTACACATggAg
Clostridiales	ACTCCTACgggAggCAgC	gCTTCTTAgTCAggTACCgTCAT
Bacteroidetes	ggTTCTgAgAggAAggTCCC	gCTgCCTCCCgTAggAgT

References

1. K. Honda, D. R. Littman, The microbiome in infectious disease and inflammation. *Annu. Rev. Immunol.* **30**, 759–795 (2012). doi:10.1146/annurev-immunol-020711-074937 Medline

2. A. Cerutti, K. Chen, A. Chorny, Immunoglobulin responses at the mucosal interface. *Annu. Rev. Immunol.* **29**, 273–293 (2011). doi:10.1146/annurev-immunol-031210-101317 Medline

3. S. Fagarasan, S. Kawamoto, O. Kanagawa, K. Suzuki, Adaptive immune regulation in the gut: T cell-dependent and T cell-independent IgA synthesis. *Annu. Rev. Immunol.* **28**, 243–273 (2010). doi:10.1146/annurev-immunol-030409-101314 Medline

4. A. J. Macpherson, D. Gatto, E. Sainsbury, G. R. Harriman, H. Hengartner, R. M. Zinkernagel, A primitive T cell-independent mechanism of intestinal mucosal IgA responses to commensal bacteria. *Science* **288**, 2222–2226 (2000). doi:10.1126/science.288.5474.2222 Medline

5. J. R. Mora, M. Iwata, B. Eksteen, S. Y. Song, T. Junt, B. Senman, K. L. Otipoby, A. Yokota, H. Takeuchi, P. Ricciardi-Castagnoli, K. Rajewsky, D. H. Adams, U. H. von Andrian, Generation of gut-homing IgA-secreting B cells by intestinal dendritic cells. *Science* **314**, 1157–1160 (2006). doi:10.1126/science.1132742 Medline

6. C. F. Ware, Network communications: Lymphotoxins, LIGHT, and TNF. *Annu. Rev. Immunol.* **23**, 787–819 (2005). doi:10.1146/annurev.immunol.23.021704.115719 Medline

7. H. S. Kang, R. K. Chin, Y. Wang, P. Yu, J. Wang, K. A. Newell, Y. X. Fu, Signaling via LTβR on the lamina propria stromal cells of the gut is required for IgA production. *Nat. Immunol.* **3**, 576–582 (2002). doi:10.1038/ni795 Medline

8. M. Tsuji, K. Suzuki, H. Kitamura, M. Maruya, K. Kinoshita, I. I. Ivanov, K. Itoh, D. R. Littman, S. Fagarasan, Requirement for lymphoid tissue-inducer cells in isolated follicle formation and T cell-independent immunoglobulin A generation in the gut. *Immunity* **29**, 261–271 (2008). doi:10.1016/j.immuni.2008.05.014 Medline

9. H. Spits, T. Cupedo, Innate lymphoid cells: Emerging insights in development, lineage relationships, and function. *Annu. Rev. Immunol.* **30**, 647–675 (2012). doi:10.1146/annurev-immunol-020711-075053 Medline

10. G. F. Sonnenberg, L. A. Monticelli, M. M. Elloso, L. A. Fouser, D. Artis, CD4$^+$ lymphoid tissue-inducer cells promote innate immunity in the gut. *Immunity* **34**, 122–134 (2011). doi:10.1016/j.immuni.2010.12.009 Medline

11. Y. Wang, E. P. Koroleva, A. A. Kruglov, D. V. Kuprash, S. A. Nedospasov, Y. X. Fu, A. V. Tumanov, Lymphotoxin beta receptor signaling in intestinal epithelial cells orchestrates innate immune responses against mucosal bacterial infection. *Immunity* **32**, 403–413 (2010). doi:10.1016/j.immuni.2010.02.011 Medline

12. L. A. Zenewicz, G. D. Yancopoulos, D. M. Valenzuela, A. J. Murphy, S. Stevens, R. A. Flavell, Innate and adaptive interleukin-22 protects mice from inflammatory bowel disease. *Immunity* **29**, 947–957 (2008). doi:10.1016/j.immuni.2008.11.003 Medline

13. N. Satoh-Takayama, C. A. Vosshenrich, S. Lesjean-Pottier, S. Sawa, M. Lochner, F. Rattis, J. J. Mention, K. Thiam, N. Cerf-Bensussan, O. Mandelboim, G. Eberl, J. P. Di Santo, Microbial flora drives interleukin 22 production in intestinal NKp46$^+$ cells that provide innate mucosal immune defense. *Immunity* **29**, 958–970 (2008). doi:10.1016/j.immuni.2008.11.001 Medline

14. M. R. Hepworth, L. A. Monticelli, T. C. Fung, C. G. Ziegler, S. Grunberg, R. Sinha, A. R. Mantegazza, H. L. Ma, A. Crawford, J. M. Angelosanto, E. J. Wherry, P. A. Koni, F. D. Bushman, C. O. Elson, G. Eberl, D. Artis, G. F. Sonnenberg, Innate lymphoid cells regulate CD4$^+$ T-cell responses to intestinal commensal bacteria. *Nature* **498**, 113–117 (2013). doi:10.1038/nature12240 Medline

15. G. Eberl, S. Marmon, M. J. Sunshine, P. D. Rennert, Y. Choi, D. R. Littman, An essential function for the nuclear receptor RORγ(t) in the generation of fetal lymphoid tissue inducer cells. *Nat. Immunol.* **5**, 64–73 (2004). doi:10.1038/ni1022 Medline

16. D. Bouskra, C. Brézillon, M. Bérard, C. Werts, R. Varona, I. G. Boneca, G. Eberl, Lymphoid tissue genesis induced by commensals through NOD1 regulates intestinal homeostasis. *Nature* **456**, 507–510 (2008). doi:10.1038/nature07450 Medline

17. A. V. Tumanov, E. P. Koroleva, X. Guo, Y. Wang, A. Kruglov, S. Nedospasov, Y. X. Fu, Lymphotoxin controls the IL-22 protection pathway in gut innate lymphoid cells during mucosal pathogen challenge. *Cell Host Microbe* **10**, 44–53 (2011). doi:10.1016/j.chom.2011.06.002 Medline

18. G. F. Sonnenberg, L. A. Monticelli, T. Alenghat, T. C. Fung, N. A. Hutnick, J. Kunisawa, N. Shibata, S. Grunberg, R. Sinha, A. M. Zahm, M. R. Tardif, T. Sathaliyawala, M. Kubota, D. L. Farber, R. G. Collman, A. Shaked, L. A. Fouser, D. B. Weiner, P. A. Tessier, J. R. Friedman, H. Kiyono, F. D. Bushman, K. M. Chang, D. Artis, Innate lymphoid cells promote anatomical containment of lymphoid-resident commensal bacteria. *Science* **336**, 1321–1325 (2012). doi:10.1126/science.1222551 Medline

19. D. J. Liepinsh, S. I. Grivennikov, K. D. Klarmann, M. A. Lagarkova, M. S. Drutskaya, S. J. Lockett, L. Tessarollo, M. McAuliffe, J. R. Keller, D. V. Kuprash, S. A. Nedospasov, Novel lymphotoxin α (LTα) knockout mice with unperturbed tumor necrosis factor expression: Reassessing LTα biological functions. *Mol. Cell. Biol.* **26**, 4214–4225 (2006). doi:10.1128/MCB.01751-05 Medline

20. A. Tumanov, D. Kuprash, M. Lagarkova, S. Grivennikov, K. Abe, A. Shakhov, L. Drutskaya, C. Stewart, A. Chervonsky, S. Nedospasov, Distinct role of surface lymphotoxin expressed by B cells in the organization of secondary lymphoid tissues. *Immunity* **17**, 239–250 (2002). doi:10.1016/S1074-7613(02)00397-7 Medline

21. G. Eberl, D. R. Littman, Thymic origin of intestinal αβ T cells revealed by fate mapping of RORγt^{+} cells. *Science* **305**, 248–251 (2004). doi:10.1126/science.1096472 Medline

22. M. B. Alimzhanov, D. V. Kuprash, M. H. Kosco-Vilbois, A. Luz, R. L. Turetskaya, A. Tarakhovsky, K. Rajewsky, S. A. Nedospasov, K. Pfeffer, Abnormal development of secondary lymphoid tissues in lymphotoxin β-deficient mice. *Proc. Natl. Acad. Sci. U.S.A.* **94**, 9302–9307 (1997). doi:10.1073/pnas.94.17.9302 Medline

23. R. D. Newberry, J. S. McDonough, K. G. McDonald, R. G. Lorenz, Postgestational lymphotoxin/lymphotoxin beta receptor interactions are essential for the presence of intestinal B lymphocytes. *J. Immunol.* **168**, 4988–4997 (2002). Medline

24. K. Suzuki, B. Meek, Y. Doi, M. Muramatsu, T. Chiba, T. Honjo, S. Fagarasan, Aberrant expansion of segmented filamentous bacteria in IgA-deficient gut. *Proc. Natl. Acad. Sci. U.S.A.* **101**, 1981–1986 (2004). doi:10.1073/pnas.0307317101 Medline

25. F. G. Kroese, E. C. Butcher, A. M. Stall, P. A. Lalor, S. Adams, L. A. Herzenberg, Many of the IgA producing plasma cells in murine gut are derived from self-replenishing precursors in the peritoneal cavity. *Int. Immunol.* **1**, 75–84 (1989). doi:10.1093/intimm/1.1.75 Medline

26. M. Muramatsu, K. Kinoshita, S. Fagarasan, S. Yamada, Y. Shinkai, T. Honjo, Class switch recombination and hypermutation require activation-induced cytidine deaminase (AID), a potential RNA editing enzyme. *Cell* **102**, 553–563 (2000). doi:10.1016/S0092-8674(00)00078-7 Medline

27. H. Tezuka, Y. Abe, M. Iwata, H. Takeuchi, H. Ishikawa, M. Matsushita, T. Shiohara, S. Akira, T. Ohteki, Regulation of IgA production by naturally occurring TNF/iNOS-producing dendritic cells. *Nature* **448**, 929–933 (2007). doi:10.1038/nature06033 Medline

28. J. H. Fritz, O. L. Rojas, N. Simard, D. D. McCarthy, S. Hapfelmeier, S. Rubino, S. J. Robertson, M. Larijani, J. Gosselin, I. I. Ivanov, A. Martin, R. Casellas, D. J. Philpott, S. E. Girardin, K. D. McCoy, A. J. Macpherson, C. J. Paige, J. L. Gommerman, Acquisition of a multifunctional IgA^+ plasma cell phenotype in the gut. *Nature* **481**, 199–203 (2012). doi:10.1038/nature10698 Medline

29. D. Tracey, L. Klareskog, E. H. Sasso, J. G. Salfeld, P. P. Tak, Tumor necrosis factor antagonist mechanisms of action: A comprehensive review. *Pharmacol. Ther.* **117**, 244–279 (2008). doi:10.1016/j.pharmthera.2007.10.001 Medline

30. See supplementary materials on *Science* Online.

31. S. I. Grivennikov, A. V. Tumanov, D. J. Liepinsh, A. A. Kruglov, B. I. Marakusha, A. N. Shakhov, T. Murakami, L. N. Drutskaya, I. Förster, B. E. Clausen, L. Tessarollo, B. Ryffel, D. V. Kuprash, S. A. Nedospasov, Distinct and nonredundant in vivo functions of TNF produced by T cells and macrophages/neutrophils: Protective and deleterious effects. *Immunity* **22**, 93–104 (2005). Medline

32. A. V. Tumanov, S. I. Grivennikov, A. A. Kruglov, Y. V. Shebzukhov, E. P. Koroleva, Y. Piao, C. Y. Cui, D. V. Kuprash, S. A. Nedospasov, Cellular source and molecular form of TNF specify its distinct functions in organization of secondary lymphoid organs. *Blood* **116**, 3456–3464 (2010). doi:10.1182/blood-2009-10-249177 Medline

33. D. J. Liepinsh, S. I. Grivennikov, K. D. Klarmann, M. A. Lagarkova, M. S. Drutskaya, S. J. Lockett, L. Tessarollo, M. McAuliffe, J. R. Keller, D. V. Kuprash, S. A. Nedospasov, Novel lymphotoxin α (LTα) knockout mice with unperturbed tumor necrosis factor expression: Reassessing LTα biological functions. *Mol. Cell. Biol.* **26**, 4214–4225 (2006). doi:10.1128/MCB.01751-05 Medline

34. J. Rothe, W. Lesslauer, H. Lötscher, Y. Lang, P. Koebel, F. Köntgen, A. Althage, R. Zinkernagel, M. Steinmetz, H. Bluethmann, Mice lacking the tumour necrosis factor receptor 1 are resistant to TNF-mediated toxicity but highly susceptible to infection by *Listeria monocytogenes*. *Nature* **364**, 798–802 (1993). doi:10.1038/364798a0 Medline

35. S. L. Erickson, F. J. de Sauvage, K. Kikly, K. Carver-Moore, S. Pitts-Meek, N. Gillett, K. C. Sheehan, R. D. Schreiber, D. V. Goeddel, M. W. Moore, Decreased sensitivity to tumour-necrosis factor but normal T-cell development in TNF receptor-2-deficient mice. *Nature* **372**, 560–563 (1994). doi:10.1038/372560a0 Medline

36. A. Tumanov, D. Kuprash, M. Lagarkova, S. Grivennikov, K. Abe, A. Shakhov, L. Drutskaya, C. Stewart, A. Chervonsky, S. Nedospasov, Distinct role of surface lymphotoxin expressed by B cells in the organization of secondary lymphoid tissues. *Immunity* **17**, 239–250 (2002). doi:10.1016/S1074-7613(02)00397-7 Medline

37. Q. Wang, G. M. Garrity, J. M. Tiedje, J. R. Cole, Naive Bayesian classifier for rapid assignment of rRNA sequences into the new bacterial taxonomy. *Appl. Environ. Microbiol.* **73**, 5261–5267 (2007). doi:10.1128/AEM.00062-07 Medline

38. C. Ubeda, Y. Taur, R. R. Jenq, M. J. Equinda, T. Son, M. Samstein, A. Viale, N. D. Socci, M. R. van den Brink, M. Kamboj, E. G. Pamer, Vancomycin-resistant *Enterococcus* domination of intestinal microbiota is enabled by antibiotic treatment in mice and precedes bloodstream invasion in humans. *J. Clin. Invest.* **120**, 4332–4341 (2010). doi:10.1172/JCI43918 Medline